Estimation of inventory and spreading of CFC-11 and CFC-12 in the North Atlantic Ocean using a three-dimensional ocean circulation model with the modified semi-prognostic method

Jun Zhao[1], Jinyu Sheng[1], Richard J. Greatbatch[1], Kumiko Azetsu-Scott[2], and E. Peter Jones[2]

[1]Department of Oceanography, Dalhousie University, Halifax, NS, Canada, B3H 4J1

[2]Ocean Sciences Division, Bedford Institute of Oceanography, Dartmouth, NS, Canada, B2Y 4A2

Corresponding author address:
Jinyu Sheng, Department of Oceanography
Dalhousie University, Halifax, NS, B3H 4J1, Canada
E-mail: Jinyu.Sheng@dal.ca

Phone: (902) 494-2718, Fax: (902) 494-2885

Short title: ESTIMATING INVENTORY AND SPREADING OF CFCS IN THE NORTH ATLANTIC

SUBMITTED TO JOURNAL OF GEOPHYSICAL RESEARCH-OCEANS ON NOV. 22, 2004

Abstract.

A three-dimensional ocean circulation model is used to examine the uptake and spreading of chlorofluorocarbons (CFCs) in the North Atlantic Ocean during the 50-year period from 1948 to 1997. The model is forced by climatological and NAO-related monthly mean surface forcing, and a realistic air-sea flux of CFCs. The novel feature of this work is the use of the modified semi-prognostic (MSP) method to compensate for systematic model bias. The MSP method is particularly well-suited to tracer studies since the adjustment to the model is made in the horizontal momentum, not the tracer equations. Use of the MSP method leads to a better representation of the Deep Western Boundary Current and a more realistic simulation of CFC concentration and spreading. The simulated inventory of CFCs in the Labrador Sea agrees reasonably well with estimates based on observations. We calculate an equatorward spreading rate of the Labrador Sea Water from the model-computed CFC effective age. The estimated spreading rate is about 1.3 cm s^{-1}, indicating slow spreading of climate anomalies from the source region in the subpolar North Atlantic to the equator. The close relationship between the NAO and the interannual variability of the model-computed overturning circulation and uptake and inventory of CFCs is also discussed.

1. Introduction

Oceans play a very important role in regulating global atmospheric concentrations of natural and anthropogenic greenhouse gases (GHG's), such as carbon dioxide (CO_2) and chlorofluorocarbons (CFCs). A significant portion of greenhouse gases added to the atmosphere dissolve in the ocean surface waters via gas exchange. Circulation (e.g. subduction) and convection can then transport the dissolved gas from the surface into the thermocline and the deep ocean [Tait et al., 2000]. Although transport between the atmosphere and ocean represents an important sink (or source) of anthropogenic gases, such as CO_2 and CFCs, reliable estimates of this sink are not presently available.

Here, we use a three-dimensional ocean circulation model to examine the major pathways, inventory and uptake of CFCs in the North Atlantic. The unique feature of our study is the use of the modified semi-prognostic (MSP) method [Eden et al., 2004; Greatbatch et al., 2004] to adjust the model for systematic bias. Since the MSP method adjusts the momentum equations of a model, and not the tracer equations, it is ideal for use in tracer studies [Zhao et al., 2004; Greatbatch et al., 2004].

CFCs were used extensively in the past as refrigerants, aerosol propellants, plastic foam blowing agents and solvents. Production of CFCs began in the early 1930s and accelerated during the following three decades as demand for these compounds grew [Bullister, 1989]. Industrial production came to a halt after the World Meteorological Organization called for a phase out of the use of these chemicals in 1987, following the realization that CFC's damage the ozone layer. Although CFC production has been eliminated for more than 15 years, the combination of the gradual release of existing stockpiles and slow removal of these compounds from the atmosphere (which is only about 1% per year via stratospheric photolysis), ensure that CFCs remain in the atmosphere at relatively high levels, and will remain so for many hundreds of years to come [Bullister, 1989].

Trichlorofluromethane (CCl_3F, CFC-11) and dichlorofluromethane (CCl_2F_2, CFC-12) are the most commonly measured CFCs in the ocean. Since CFC-11 and CFC-12 are inert in seawater, they are widely used as passive tracers for interpreting field measurements

and verifying numerical simulations [Rhein, 1994; England, 1995; Azetsu-Scott et al., 2003; Beismann and Redler, 2003; Haine et al., 2003; Kieke et al., 2004], and can be used to identify different water masses and water mass pathways, e.g., in association with the meridional overturning circulation. CFCs have been measured as part of several multi-purpose research programs, including the Transient Tracer in the Ocean [Williams, 1986], North and Tropical Atlantic Studies [Weiss et al., 1985], Western Boundary Exchange [Smethie, 1993], and World Ocean Circulation Experiments [Smethie, 1999; Azetsu-Scott et al., 2003]. The uptake and redistribution of CFCs in the ocean are strongly linked with physical processes such as convection, mixing, and air-sea fluxes. Comparisons between observed and model-calculated CFC concentrations can thus be used to validate physical processes in models, examples being the parameterization of sub-grid scale mixing [England et al., 1994; Haine and Richards, 1995; Robitaille and Weaver, 1995; Beismann and Redler, 2003], ocean ventilation [Dixon et al., 1996; Haine et al., 2003]; surface thermohaline forcing [England and Hirst, 1997]; the formation rate of Labrador Sea Water [Böning et al., 2002]; and small-scale convection beneath sea ice [Caldeira and Duffy, 1998].

Dutay et al. [2002] recently compared the simulated CFC fields produced by 13 different global ocean models, with model horizontal resolutions ranging from 0.5° to 5°. They found that the models have difficulty in simulating realistically the CFC distribution in the region of the Deep Western Boundary Current (DWBC) in the North Atlantic. In fact, poor representation of the CFC concentration in the DWBC region is a common problem in models of the North Atlantic. England and Holloway [1998] suggested that the poor model performance of resolving the CFC-bearing cores within the DWBC is due to the fact that the simulated currents in the deep North Atlantic Ocean are too weak and too broad compared to the real ocean. On the other hand, Zhao et al. (2004) showed that using the MSP method led to a significant improvement in the simulation of the DWBC and associated CFC distributions in a model of the North Atlantic, an issue we explore further in the study presented here.

The paper is organized as follows. Section 2 presents the ocean circulation model and

discusses the modified semi-prognostic method. Section 3 presents the model results and compares the simulated CFC distributions with observations made in the North Atlantic. Section 4 is a summary and conclusion.

2. The Ocean Circulation Model and the Modified Semi-Prognostic Method

2.1 Model Description

We use the three-dimensional z-level ocean model known as FLAME (Family of Linked Atlantic Model Experiments [Dengg et al., 1999]). The model domain covers the Atlantic Ocean from 18°S to 70°N, using the ETOPO5 bathymetry, which is a gridded elevation/bathymetry compiled by the U.S. National Geophysical Data Center (NOAA). The model horizontal resolution is 4/3° in longitude and 4/3°cosϕ in latitude (ϕ denoting latitude). There are 45 unevenly spaced z-levels in the vertical, with a thickness of 10 m in the top z-level and a smooth increase to 250 m below 2000 m. The model uses the Quicker advection scheme (as in Eden et al. [2004]), and since it does not resolve eddies, instead employs the isopycnal mixing scheme of Redi [1982] and the eddy-induced tracer advection parameterization of Gent and McWilliams [1990]. The isopycnal diffusivity is set to 2×10^7 cm^2 s^{-1} in the near surface layers, decaying with depth to 0.5×10^7 cm^2 s^{-1} below 4000 m. The thickness diffusivity is specified to have half the magnitude of the isopycnal diffusivity. There is also a background horizontal diffusivity (viscosity) that is set to 10^6cosϕ cm^2 s^{-1} (10^8cosϕ cm^2 s^{-1}). The turbulent kinetic energy (TKE) scheme of Gaspar et al. [1990] is used to calculate the vertical eddy diffusivity and viscosity, the parameters used for the TKE scheme being identical to those in Oschlies and Garcon [1999]. We follow Beismann and Redler [2003] and set the flow across the model northern boundary at 70°N and the Strait of Gibraltar to zero, with narrow restoring zones for temperature and salinity (see Section 2.4). Along the model southern open boundary at 18°S, the depth-mean flow is prescribed based on a simple Sverdrup-relation, with temperature and salinity restored to climatological values. The model also uses the bottom boundary layer parameterization (BBL) of Beckmann and Döscher [1997], and a

simple parameterization for the effect of sea-ice (the surface forcing for heat and salt is turned off if the SST is below freezing point).

2.2 The Modified Semi-Prognostic Method (MSP)

The MSP method is a modification of the original semi-prognostic method (OSP) introduced by Sheng et al. [2001] in order to eliminate the damping effect on small scales (e.g. the mesoscale) of the OSP method. Both the MSP and OSP methods were developed to provide a simple way to adjust a model to correct for systematic error (see Greatbatch et al. [2004] for a comprehensive overview). Both methods are closely related to the "pressure-correction method" of Bell et al. [2004].

In the MSP method, the model's hydrostatic equation is replaced by

$$\frac{\partial p}{\partial z} = -g\rho_m + g(1-\alpha)\Big\langle \rho_m - \rho_c \Big\rangle \tag{1}$$

where ρ_m is the model-computed density, ρ_c is an input density, α is a linear combination coefficient between 0 and 1, and $\langle\ \rangle$ represents a filtering operator (the OSP uses (1) without filtering). ρ_c and ρ_m are given by

$$\rho_c = \rho(\theta_c, S_c, P_{ref}), \tag{2}$$

and

$$\rho_m = \rho(\theta_m, S_m, P_{ref}) \tag{3}$$

where P_{ref} is a reference pressure (depending only on depth), θ_c and S_c are climatological potential temperature and salinity, θ_m and S_m are the model-calculated potential temperature and salinity, and $\rho = \rho(\theta, S, p)$ is the equation of state for sea water. When $\alpha = 1$, the model is purely prognostic and the climatological density plays no role in the model dynamics. When $\alpha = 0$, then with the OSP (no filtering in (1)), the model is purely diagnostic, and the model temperature and salinity fields become passive tracers. (See Zhai et al. (2004) for an example using (1) with $\alpha = 0$ but using a spatial filter for $\langle\ \rangle$ - the so-called "semi-diagnostic" method.)

As shown in Sheng et al. [2001], the above procedure is equivalent to adding a forcing term to the horizontal momentum equation [see also Greatbatch et al., 2004]. This can

be seen by decomposing the model pressure variable p into two parts:

$$p = p^* + \hat{p}, \tag{4}$$

where p^* is the physical pressure satisfying

$$\frac{\partial p^*}{\partial z} = -g\rho_m, \tag{5}$$

with $p^* = g\rho_o\eta$ at the sea surface, and $\hat{p}$ is a pressure correction satisfying

$$\frac{\partial \hat{p}}{\partial z} = g(1-\alpha)\Big\langle \rho_m - \rho_c \Big\rangle. \tag{6}$$

with $\hat{p} = 0$ at the sea surface. (Here, η is sea surface height and ρ_o is a representative density for sea water.) Substitution of (4) into the horizontal momentum equation yields

$$\frac{\partial \vec{u}}{\partial t} = -\frac{1}{\rho_o}\nabla_h p^* - \frac{1}{\rho_o}\nabla_h \hat{p} + \ldots, \tag{7}$$

where $\vec{u}$ is the horizontal velocity vector and ∇_h is the horizontal gradient operator. Therefore, the semi-prognostic method is equivalent to adding a forcing term $(-\frac{1}{\rho_o}\nabla_h\hat{p})$ to the model horizontal momentum equations. It is important to note that the temperature and salinity equations are unchanged by the method [Greatbatch et al. 2004], and it is for this reason the semi-prognostic method is well-suited for use in tracer studies [e.g., Zhao et al., 2004]. For the same reason, the semi-prognostic method makes no compromise to the requirement that the flow be primarily in the neutral tangent plane in the ocean interior.

Eden et al. [2004] introduced modified versions of the OSP depending on the form of filtering used for $\langle\ \ \rangle$ in (1). In the smoothed semi-prognostic method, the filtering operator $\langle\ \ \rangle$ in (1) represents spatial filtering and the correction term $g(1-\alpha)\langle\rho_m - \rho_c\rangle$ is applied only on large spatial scales. In the mean semi-prognostic method, the correction term is computed using only annual means for ρ_c and ρ_m to avoid damping or distorting physical processes with time scales shorter than annual. In the tapered semi-prognostic method, the correction term is tapered to zero near sloping bottom topography to prevent spurious interaction with the model bottom topography. In the present study, the mean

and tapered semi-prognostic methods are combined and used to simulate circulation and CFC distributions in the North Atlantic Ocean. (It should be noted that the use of tapering is not essential to obtain the model results we show.) The value of α is set to 0.5. The reader is referred to Sheng et al. [2001] and Greatbatch et al. [2004] for a more detailed discussion on the choice of α.

2.3 Model Forcing and Experimental Design

Two types of model forcing are used in this study. The first type is the climatological monthly mean forcing (CLIM), which includes the monthly mean wind stress and net heat flux taken from 6-hourly analysis data produced by the European Centre for Medium-range Weather Forecast (ECMWF) for the period 1986-1988 [Barnier et al., 1995]. The second type of model forcing (CLIM+NAO) is the combination of the climatological monthly mean forcing mentioned above and monthly mean forcing associated with the NAO constructed by Eden and Jung [2001][1]. Eden and Jung's NAO-related forcing is based on the regression of anomalous fields of monthly surface heat flux and wind stress computed from the NCEP-NCAR reanalysis [Kalnay et al., 1996] against the monthly NAO index for the period 1958-97. The NAO-related forcing for each month from 1948 to 1997 is then reconstructed by multiplying the associated regression patterns of surface heat flux and wind stress by the monthly NAO index [Eden and Jung, 2001]. The NAO index (see Figure 2) used to construct Eden and Jung's NAO-related forcing is defined as the difference in normalized sea level pressure anomalies between Azores and Iceland [Rogers, 1984]. Eden and Willebrand (2001) have noted the dominance of the NAO as a forcing for variability in the North Atlantic meridional overturning circulation on time scales from interannual to interdecadal.

The sea surface boundary condition for the net heat flux used in this study includes

[1]The NAO is the North Atlantic Oscillation - see Greatbatch (2000) and Hurrell et al. (2003).

a relaxation to an input sea surface temperature (SST_i), as given by Barnier et al. [1995]:

$$Q = Q_i + \beta(SST_m - SST_i) \tag{8}$$

where Q_i is the input surface heat flux, and SST_m is the model-calculated sea surface temperature. In the CLIM forcing case, Q_i and SST_i are the climatological monthly mean surface heat flux and sea surface temperature, respectively, with Q_i replaced by the sum of the climatological and NAO-related monthly mean surface heat flux in the CLIM+NAO forcing case. The second term in (8) is a correction in the form of restoring to SST_i, with a temporally and spatially varying time scale $1/\beta$, determined from a linearization of the bulk parameterization of surface heat flux components:

$$\beta = \left.\frac{\partial Q}{\partial(SST)}\right|_{SST_{clim}} \tag{9}$$

where SST_{clim} is the climatological monthly mean SST. The time scale $1/\beta$ used in this study is taken from Barnier et al. [1995]. The sea surface salinity is restored towards a combined climatology of Levitus and Boyer [1994] and Boyer and Levitus [1997] on a time scale of 15 days. The relaxation values for temperature and salinity used for SST_i in (8) and along the northern boundary and at the Straits of Gibraltar are also taken from the combined climatology of Levitus and Boyer [1994] and Boyer and Levitus [1997], except for the relaxation zone near the northern boundary where the relaxation values are taken from a dataset that was used in the DYNAMO (DYnamic North Atlantic MOdels) project [DYNAMO-group, 1997] to include the effect of water mass formation in the Greenland Sea. The method for specifying the flux of CFC-11 and CFC-12 at the sea surface is described in Section 2.5.

Three numerical experiments are conducted to examine the inventory and spreading of CFCs and associated interannual variability in the North Atlantic Ocean. The model in the first experiment is forced by the combination of climatological and NAO-related monthly mean forcing, using the modified semi-prognostic method (Exp NAO-sp, control run). The model in the second and third experiments is forced by the climatological monthly mean forcing only. The second experiment is an uncorrected, prognostic model run ($\alpha = 1$ in (1); Exp CLIM-pp), while in the third experiment (Exp CLIM-sp), the

modified semi-prognostic method is used. In each case, the model is spun up for 20 years by forcing with the climatological monthly mean forcing. The 20-year spin-up allows the ocean circulation model to reach a state of quasi-equilibrium under the applied forcing [Döscher et al., 1994; Böning et al., 1996]. After the 20-year spin-up, the model is integrated with zero initial concentrations of CFC-11 and CFC-12 specified everywhere in the model domain. Since the atmospheric concentrations of CFCs were very low (near zero) before 1950, numerical simulations of CFC-11 and CFC-12 in each experiment are carried out for the 50-year period from 1948 to 1997.

2.4 Net CFC Flux at the Sea Surface

The net flux of CFCs at the sea surface F is parameterized in terms of a CFC concentration difference between the air and sea surface:

$$F = K(C_{sat} - C_w) \tag{10}$$

where K is the gas transfer velocity known as the piston velocity, C_w is the modeled CFC concentration at the sea surface, and C_{sat} is the saturated CFC concentration at the sea surface defined as AC_a, in which C_a is the dry air mole fraction in the atmosphere and A is the solubility coefficient of CFCs at the sea surface [Warner and Weiss, 1985]. Due to the rapid mixing rate of CFCs in the lower atmosphere, the spatial atmospheric distribution is almost uniform in the northern and southern hemispheres (Figure 1). In this study, we follow Walker et al. [2000] and set C_a to be uniform in each hemisphere poleward of 10° latitude, using temporal values from the reconstructed annual mean mole fraction of C_a at 41°S and 45°N. Between 10°N and 10°S, the values are linearly interpolated [Dutay et al., 2002].

We follow Beismann and Redler [2003] and use the wind-speed dependent gas transfer velocity formulation proposed by Wanninkhof [1992]:

$$K = 0.39(S_c/660)^{-0.5} U_{wind}^2 \tag{11}$$

where U_{wind} is the climatological monthly mean wind speed at 10 m above the sea surface, S_c is the Schmidt number in the water, which is the ratio of kinetic viscosity

to molecular diffusivity. Wanninkhof [1992] fitted polynomial approximations to S_c for a range of environmental gases, including CFC-11 and CFC-12. Eq. (11) is exactly the same parameterization as used by Beismann and Redler [2003], which allows us verify our model against their study. It should be noted that no specification of CFC concentration is made at the northern closed boundary, the Mediterranean Sea, and the southern open boundary, due to a lack of observed data.

3. Model Results

3.1 Time-Mean Circulation and Interannual Variability

We first examine the time-mean circulation calculated from the 50-year (1948-1997) model run in Exp NAO-sp (control run). The time-mean volume transport streamfunction is shown in Figure 3 and is typical of that found in z-coordinate ocean models of comparable resolution [e.g., Eden and Willebrand, 2001; Beismann and Barnier, 2004]. The time-mean transport of the North Atlantic subtropical gyre is about 35 Sv (1 Sv=10^6 m^3 s^{-1}), which is consistent with the flat-bottomed Sverdrup relation [Leetmaa et al., 1977]. The strength of the model-calculated subpolar gyre in the North Atlantic is about 20 Sv. The time-mean meridional overturning streamfunction (Figure 4) is characterized as a main thermohaline cell centered at the depth of 1000 m, with a northward flow in the top 600 m and a southward flow beneath 1300 m. The maximum strength of the meridional overturning is about 18 Sv, which is again in the typical range of the meridional overturning transport produced by other z-level North Atlantic models using similar horizontal resolutions [Döscher and Redler, 1997; Böning et al., 1996].

The dominant pattern of the atmospheric circulation variability over the North Atlantic is the North Atlantic Oscillation (NAO). Changes in the NAO significantly affect water properties and circulation in the region [Eden and Willebrand, 2001; Visbeck et al., 2003]. Although some ocean responses, such as the sea surface temperature and mixed layer depth, are local and rapid, the large-scale horizontal and overturning ocean circulation can take several years, even decades to adjust to changes in the forcing [Eden and Greatbatch, 2003; Visbeck et al., 2003]. The role of the NAO-related forcing in

our model can be seen in Figure 5, where we compare the strength of the annual mean overturning streamfunction at 48°N and 1000 m depth in experiments NAO-sp and CLIM-sp. (The only difference between these two experiments is that the model is driven by the combination of climatological and NAO-related forcing in Exp NAO-sp and by the climatological forcing only in Exp CLIM-sp). In Exp NAO-sp, there is significant interannual variability in the annual mean overturning strength, in the range between 14 Sv and 17.5 Sv, in good agreement with Eden and Willebrand [2001] and Eden and Jung [2001]. By comparison, the annual mean overturning strength in the CLIM-sp case has much smaller interannual variability of less than 1 Sv during the first 20 year simulations, and reaches a constant value of about 15.5 Sv in the last 30 years of the simulation (Figure 5). Therefore, the NAO-related forcing plays a dominant role in generating the interannual variability of the meridional overturning circulation (MOC) in the model, while the internal variability of the model (presumably associated with model drift) plays only a secondary role.

To further demonstrate the role of NAO-related forcing in the interannual variability of the MOC, we compare the low-pass filtered (5-point moving average) winter-mean (JFM) NAO index with the unfiltered anomaly of the annual mean overturning streamfunction at 48°N and 1000 m depth from Exp NAO-sp (Figure 6). The anomaly is defined as the difference between experiments NAO-sp and CLIM-sp shown in Figure 5. The variability of the MOC strength is strongly correlated with the low-pass filtered winter-mean NAO index (r=0.89), with a phase lag of about 2 years (NAO leading). There is a decrease of the meridional overturning of approximately 1.5 Sv in the late 1960s in response to the persistent negative phase of NAO at that time, and a 2 Sv increase of the overturning streamfunction in early the 1990's in response to the persistent positive phase of the NAO during this period. The phase lag of about 2 years is consistent with the finding of Eden and Greatbatch [2003], using essential the same model as here, but with the NAO-forcing specified using a random number generator.

3.2 Impact of Using the Modified Semi-Prognostic Method

We next examine the impact of using the modified semi-prognostic (MSP) method. Previous studies by Sheng et al. [2001] and Eden et al. [2004] demonstrate that the use of the semi-prognostic method in eddy-permitting ocean circulation models leads to a significant improvement of the numerical simulation of the Gulf Stream and the North Atlantic Current. Zhao et al. [2004] showed that the use of the MSP method in a $4/3° \times 4/3° \cos\phi$ non-eddy-permitting ocean circulation model also leads to improvement in the representation of the Deep Western Boundary Current (DWBC), which, in turn, has a positive impact on the simulation of CFC-12.

We begin by comparing the time-mean currents at 200 m calculated from the 50-year model runs in Exp CLIM-pp and Exp CLIM-sp (Figure 7). The only difference between these two experiments is that the CLIM-pp case is a prognostic (uncorrected) model run, while the CLIM-sp case uses the MSP method (both models use climatological forcing only). The Gulf Stream produced by the prognostic model (Figure 7a) is too broad and the main pathway of the North Atlantic Current (NAC) also differs significantly from the observations. In fact, observational studies show that the NAC flows first northward along the outer flank of the Grand Banks and then turns east at about 52°N in the "northwest corner" [Lazier, 1994]. The use of the MSP method improves significantly the Gulf Stream and the NAC (Figure 7b), particularly in the northwest corner region. The model using the MSP method also generates a more realistic subpolar circulation in the Labrador Sea and Labrador Basin, in comparison with the prognostic model run.

Figure 8 compares the time-mean currents at 1500 m depth in the two experiments, which further demonstrates the advantage of using the MSP method over a prognostic, uncorrected model. The MSP method produces a well-defined sub-surface equatorward flow (i.e., DWBC) that runs around the southern tip of the Grand Banks and then flows southwestward along the continental slope of the Grand Banks and Scotian Shelf to the subtropical Atlantic Ocean (Figure 8b). In comparison, the prognostic model does not reproduce the DWBC well in the northwest Atlantic Ocean (Figure 8a). Instead, the prognostic model has an equatorward flow that runs first eastward to the Mid-Atlantic

Ridge and then turns southwest in the ocean interior. The flow produced by the prognostic model is too broad and is removed from the western boundary to the north of 30°N.

We next compare the simulated CFC-11 distribution in February 1990 in experiments CLIM-pp and CLIM-sp (Figure 9). As mentioned earlier, the MSP method is adiabatic and hence well-suited for tracer simulations in the ocean. The model results in both experiments generate high CFC concentrations in the Labrador Sea in response to the winter convection in the region. The high concentrations subsequently leak out to the rest of the North Atlantic, but in rather different ways in each case. In the prognostic model (i.e., Exp CLIM-pp), the DWBC becomes detached from the continental slope, resulting in a high-concentration tongue in the basin interior (Figure 9c). In the MSP run (i.e., Exp CLIM-sp), the DWBC follows the continental slope, leading to a rather different pattern in which much higher CFC-11 concentrations are now found near the continental slope (Figure 9d).

Figure 10 compares simulated and observed CFC-11 concentrations along the WOCE hydrographic/tracer section A20 at 52°W (a similar figure is shown in Zhao et al. [2004], but for CFC-12). The observed CFC-11 concentrations made in July/August of 1997 have three distinct sub-surface CFC-enriched water cores (see Smethie et al. [1999] for details). The shallowest observed high-concentration core, about 280 m depth and between 16°N to 39°N, is associated with subtropical mode water (Figure 10a). The two deeper sub-surface observed maxima are close to the continental slope, with one centered at about 1500 m north of 30°N associated with Labrador Sea Water (LSW) and the other at about 4000 m near the bottom of the continental slope, associated with the deep overflows. There is also a CFC-11 minimum at about 1000 m associated with Upper Circumpolar Water (UCW), which is far from its source region (the Southern Ocean) and hence has a low CFC concentration. Both the prognostic and MSP model runs reproduce reasonably well the overall features of the CFC-11 distribution (Figures 10b and c). On the negative side, both the model runs show too strong a minimum in association with UCW (apparently the semi-prognostic method is not able to correct for this error) and both are missing the deep maximum associated with the overflows. On the other hand, both the methods

reproduce the sub-surface maximum associated with LSW [Zhao et al., 2004], and it is here that the major difference between the two model runs is found. In particular, the sub-surface CFC-11 maximum produced by the MSP method is close to the continental slope, while the maximum produced by the prognostic model is away from the slope (as in Figure 9b). By comparing the simulated and observed CFC-12 concetrations along the same WOCE section, Zhao et al. [2004] also came to the conclusion that use of the MSP method leads to a better simulation of CFC distribution in the North Atlantic than a prognostic (uncorrected) model. It should be noted that the observed distributions of CFC-11 and CFC-12 in the North Atlantic are similar, with the observed CFC-12/CFC-11 ratio to be about 0.52 ± 0.04 for the entire Labrador Sea.

3.3 Interannual Variability in the CFC Uptake and Inventory

It has long been recognized [e.g., Smethie and Fine, 2001] that winter convection in the Labrador and Greenland Seas plays a major role in controlling the CFC uptake in the North Atlantic. The rapid mixing of CFC-rich surface waters with CFC-deficient sub-surface waters caused by winter convection reduces the sea surface CFC concentration, which, in turn, leads to large CFC fluxes at the sea surface. To demonstrate the model capacity to simulate the CFC uptake associated winter convection, we integrate the annual mean air-sea flux of CFC-11 (pmol s^{-1}) over the area of the Labrador Sea (43°W-60°W, 49°N-64°N) in experiments NAO-sp and CLIM-sp. Figure 11 shows that the uptake of CFC-11 in the Labrador Sea is relatively small in the model before 1950, but increases significantly during the 30-year period from 1960 to 1990 in both experiments. In fact, the region-integrated air-sea flux of CFC-11 in 1990 is about 10 times larger than that in 1960. This 10-fold increase is consistent with the increase in the atmospheric CFC-11 concentration during the same 30-year period (Figure 1). After 1990, the region-integrated air-sea flux of CFC-11 gradually decreases (Figure 11), explained by the fact that the atmospheric concentration of CFC-11 levels off after 1990 (Figure 1).

When the NAO-related forcing is added to the climatological forcing (i.e., Exp NAO-sp), the surface flux of CFC-11 over the Labrador Sea shows significant interannual

variability (Figure 11). To determine the relationship between the interannual variability in the surface flux of CFC-11 and the atmospheric forcing, we compare the winter-mean NAO index with the normalized surface flux anomaly, defined as the difference in the surface flux of CFC-11 between experiments NAO-sp and CLIM-sp normalized by the values in Exp CLIM-sp (Figure 12). The normalized surface flux anomaly is highly correlated with the winter NAO index, with a correlation coefficient of about 0.95 and zero phase lag, indicating the strong connection between CFC uptake and the winter-mean NAO index in the model. The strong connection between CFC uptake and the winter-mean NAO index is because deep convection in the model is stronger in the Labrador Sea in the positive NAO phase compared to the negative NAO phase, as shown, for example, by Eden and Willebrand (2001).

Azetsu-Scott et al. [2003] recently estimated CFC-12 inventories in the Labrador Sea in the 1990s based on field measurements along the WOCE AR7W section (shown in Figure 3). They calibrated their estimates using the inventory estimate made directly from a basin wide survey in 1997 [Azetsu-Scott et al., 2004]. They found the CFC-12 inventory in the Labrador Sea is about 7.56×10^6 mol in 1997, with an increase in the CFC-12 inventory of about 0.36×10^6 mol year^{-1} during the 1990s (Figure 13a). To validate the model performance, we calculate the annual mean CFC-12 inventory in the Labrador Sea from the model in experiments CLIM-sp and NAO-sp (Figure 13a). The model-calculated CFC-12 inventories are comparable to, or slightly higher than, the observation-based estimates made by Azetsu-Scott et al. [2003]. The model-calculated CFC-12 inventory in 1997 in the Labrador Sea is about 8.11×10^6 mol in Exp NAO-sp and about 7.87 $\times10^6$ mol in Exp CLIM-sp, agreeing reasonably well with Azetsu-Scott et al.'s estimate for the same year. The model-calculated CFC-12 inventories in the Labrador Sea increase with time at a rate of about 0.025×10^6 mol year^{-1} before 1970 and about 0.27×10^6 mol year^{-1} (about 10 times higher) from 1975 to 1995.

The inventory anomaly, defined as the difference in the annual mean inventory in the Labrador Sea between experiments NAO-sp and CLIM-sp, is compared with the low-pass filtered winter-mean NAO index in Figure 13b. The model-calculated inventory anomaly

has maximum correlation (r = 0.86) with the low-pass filtered NAO index at a time lag of about 1 year, with the NAO leading. Böning et al. [2002] found a similar one year lag between Labrador Sea Water renewal and the winter-mean NAO index in a model similar to ours, but with eddy-permitting resolution. Figure 13b demonstrates that the CFC-12 inventory anomaly in the Labrador Sea is relatively small during the negative NAO phase from 1955 to 1970 when deep convection in the model is relatively less active in the Labrador Sea. In comparison, the model-calculated CFC-12 inventory anomaly is significantly larger and positive during the positive NAO years from 1974 to 1980 and from 1990 to 1997, when convection was relatively active. (See Eden and Willebrand [2001] for discussion of the relationship between the NAO and convective activity in the Labrador Sea in the model.)

3.4 The Spreading of Labrador Sea Water

North Atlantic Deep Water (NADW) is formed by winter convection in the Labrador and Greenland Seas, and has the signature of the CFC concentration at the time the new NADW water mass was formed. As a result, the CFC distribution in the ocean has useful information about the spreading of NADW (in particular the MOC). The spreading rate of NADW, as it flows from the source region in high latitudes to the equator, can be estimated from the ratio of the distance from the source region to the age of the water mass.

Ventilation age is defined as the time elapsed since the water last contacted the atmosphere. The partial pressure CFC (pCFC) method and the CFC-11/CFC-12 ratio method are two common approaches used in the community to estimate ventilation age from observed CFC concentrations in the ocean [Fine et al., 1988; Weiss et al., 1985]. The pCFC age method is to convert the observed oceanic CFC concentration to an atmospheric concentration using the temperature and salinity dependent solubility function, and determine the date at which the observed atmospheric concentration is the same as the converted atmospheric concentration. The CFC-11/CFC-12 ratio method is to determine the water age by converting the oceanic ratio of CFC-11/CFC-12 of the

water sample to the atmospheric ratio and comparing it with the time history of the atmospheric ratio. Although the CFC-11/CFC-12 ratio method has an advantage of estimating the age of the CFC-bearing component, it can only be used for water formed before 1975 [Smethie et al., 2000].

To determine the pCFC-11 age from the model, we calculate the annual mean CFC-11 concentration in 1997 on the isopycnal surface $\sigma_o = 27.8$ kg m^{-3}, corresponding to LSW, using output from experiment CLIM-sp. This isopycnal surface corresponds to the layer at which both CFC-11 and CFC-12 reach a maximum within the LSW layer. We estimate the age of the water mass on this isopycnal surface by comparing the annual mean CFC-11 concentration calculated above with the time series of the annual mean sea surface CFC-11 concentration averaged over the source region (43°W-60°W, 49°N-64°N). The model-calculated ventilation age in the Labrador Sea and Basin is about 14 years (Figure 14), which is the youngest in comparison with computed water ages over other regions of the North Atlantic. (The white area in the central Labrador Sea indicates the isopycnal surface outcrop to the sea surface). Over the tropical and equatorial regions, the computed ventilation age of the LSW is 30 years or older. In addition, the model-calculated CFC-11 water age is younger over the western basin than over the eastern basin of the North Atlantic, due mainly to the DWBC transport of newly formed NADW along the western boundary.

To estimate propagation and storage of climate anomalies in the deep western North Atlantic Ocean, Fine et al. [2002] introduced the concept of CFC effective age, defined as an average age for the water mass since leaving the source region. The CFC effective age can be calculated by subtracting a relic age from the pCFC age to remove the apparent age caused by entrainment and dilution in the source region and the residence time of the water mass before leaving the formation region. Figure 15 shows the CFC-11 effective age on the isopycnal surface σ_0=27.78 kg/m^3 estimated by Fine et al. [2002] from observed CFC-11 concentrations collected in the 1990s. To compare our model results with Fine et al.'s CFC-11 effective age, we subtract the relic age of 14 years for the LSW, which is comparable to 15 years used in Fine et al., from the model-calculated pCFC-11 age

shown in Figure 14. The overall distribution of the model calculated CFC-11 effective age in the North Atlantic produced by the MSP method (Exp CLIM-sp; Figure 16a) agrees qualitatively with the observation estimates by Fine et al. (Figure 15).

The model-calculated CFC-11 effective age in the MSP case (Figure 16a) is youngest and near zero in the regions of the Labrador Sea, Labrador Basin and Norwegian Basin, and older than 20 years over the eastern basin of the North Atlantic to the south of 30°N. Along the pathway of the DWBC, the CFC-11 effective age varies from about 10 years near 45°N to 26 years at the equator.

Figure 16b shows the CFC-11 effective age produced by the prognostic (uncorrected) model in experiment CLIM-pp, the overall distribution of which is comparable to that produced by the MSP method. The major difference between the prognostic and MSP cases is that the effective age along the pathway of the DWBC is about 10 years older in the prognostic case than that in the MSP case and the prognostic results agree less well with the observation estimates of Fine et al. [2002]. These results demonstrate, once again, the advantage of using the MSP method over a prognostic (uncorrected) model in simulating circulation and tracers in the ocean.

Based on the model-calculated CFC-11 effective age, we calculate the equatorward spreading rate of the DWBC in Exp CLIM-sp. The spreading rate is about 1.3 cm s^{-1}, which agrees reasonably well with the earlier estimates of 1-2 cm s^{-1} based on CFC observations [Doney and Jenkins, 1994; Smethie et al., 2000; Fine et al., 2002]. It should be noted that the typical velocity of the DWBC estimated from sparse current-meter measurements along the North American continental slope is about 10-20 cm s^{-1} on average [e.g., Johns et al., 1993; Schott et al., 1993], which is considerably higher than the spreading rate estimated above. The main reason for the difference between the spreading rate derived from the CFC age and the direct velocity measurement is that the former estimates gives an effective spreading rate, which includes the effects of mixing and recirculation. Bower and Hunt [2000] also obtained a consistent spreading rate for NADW in the range 0.6-1.4 cm s^{-1} based on their study of RAFOS floats launched between the Grand Banks and Cape Hatteras in 1994-1995. The float observations reveal that the

pathway is not directed from the source region to the equator along the western boundary. The tracks of floats show the LSW diverted from the western boundary into the interior at the crossover region where the DWBC encounters the Gulf Stream. Then the LSW is mixed with older water and is returned back to the western boundary associated with recirculation gyres.

4. Conclusions

A three-dimensional, primitive-equation ocean circulation model (FLAME) has been used to simulate the large-scale circulation and CFC-11 and CFC-12 distributions in the North Atlantic for the 50-year period from 1948-1997. The model domain covers the Atlantic Ocean from 18°S to 70°N, with a horizontal resolution of $4/3^\circ \times 4/3^\circ \cos\phi$, with ϕ denoting latitude. We use the modified semi-prognostic (MSP) method developed by Eden et al. [2004] in this study. The MSP method provides a simple way to adjust an ocean circulation model to correct for systematic error by adding a forcing term to the model horizontal momentum equations [Sheng et al., 2001; Greatbatch et al., 2004], and is closely related to the "pressure-correction method" of Bell et al. [2004]. The MSP method is adiabatic, leaving the temperature and salinity equations unadjusted [Greatbatch et al., 2004]. As a result, the method is well-suited for use in tracer studies in the ocean. We have seen in this study that the MSP method leads to an improvement in the simulation of the North Atlantic in a non-eddy resolving model, particularly the North Atlantic Current as it flows first northward along the Grand Banks and then turns to the east at the "northwest corner" [Lazier, 1994]. The use of the MSP method also produces a well-defined sub-surface equatorward flowing Deep Western Boundary Current (DWBC) that runs around the Grand Banks and then along the western continental slope. It is the improvement in the simulation of the DWBC in the MSP case compared to the (uncorrected) prognostic model run that is important for the improved simulations of CFC-11 and CFC-12 concentration found in this study (see also Zhao et al. [2004]).

Forced by combined climatological and NAO-related monthly mean surface forcing, the ocean circulation model using the MSP method simulates interannual variability in

the strength of the MOC in close agreement with Eden and Jung [2001] and Eden and Willebrand [2001]. The interannual varying strength of the MOC is highly correlated with the low-pass filtered winter-mean NAO index (r=0.89). The phase lag is about 2 years with the NAO index leading, in agreement with the work of Eden and Greatbatch [2003]. By introducing CFC-11 and CFC-12 as passive tracers in the model, the simulated sea surface flux and inventory of CFC-11 and CFC-12 in the Labrador Sea region also have significant interannual variability. The normalized anomaly of the annual mean surface flux of CFC-11 is highly correlated to the winter-mean NAO index, with a correlation coefficient of r=0.95 and zero phase lag. This indicates that the surface flux of CFC responds quickly to the variability in the atmospheric forcing. During positive NAO index period, intensive convection occurs in the Labrador Sea region, which causes high air-sea CFC flux. The model-calculated CFC-12 inventory in the Labrador Sea is relatively small before 1965, but increases significantly after 1975 at a rate of roughly 0.27×10^6 mol year^{-1}. The model-calculated CFC-12 inventory in the Labrador Sea is about 7.87 $\times10^6$ mol in 1997, in good agreement with the observation estimate of 7.56 $\times10^6$ mol made by Azetsu-Scott et al. [2003]. The model-calculated CFC-12 inventory also has significant interannual variability that has an intimate relation with the low-pass filtered NAO index (r=0.86, 1 year lag, NAO index leading).

We estimate the DWBC spreading rate from the CFC-11 effective age calculated from simulated CFC-11 concentrations on the isopycnal surface σ_0 = 27.8 kg m^{-3}, corresponding to Labrador Sea Water (LSW). By subtracting a "relic" age of 14 years, which corresponds to the time duration for the LSW to remain in the source region, the model-calculated CFC-11 effective age on the isopycnal surface is about 25 years near the equator. The model-calculated age distribution agrees reasonably well with the observation-based estimates made by Fine et al. [2002]. Based on the CFC model-calculated CFC-11 effective age, we estimate the equatorward DWBC spreading rate to be about 1.3 cm s^{-1}, which is in the same range as the spreading rate derived from floats of 0.6-2.0 cm s^{-1} [e.g., Bower and Hunt, 2000]. The effective spreading rate is more than 10 times slower than the direct current measurements of the DWBC. This is

not surprising since the spreading rate takes into account the effect of recirculation and mixing, which reduce the spreading of climate anomalies from the source region in the subpolar North Atlantic to the equator.

Acknowledgments

We are very grateful to Carsten Eden for his efforts in setting up the FLAME model for us. We also wish to thank Jens-Olaf Beismann, Monika Rhein and Dagmar Kieke for helpful discussions. This project is supported by the Canadian SOLAS (Surface Ocean-Lower Atmosphere Study) and CLIVAR Research Networks funded by NSERC, CFCAS and CICS. RJG and JS are also supported by the NSERC/MARTEC/MSC Industrial Research Chair, and EPJ is supported by the Panel on Energy Research and Development (Canada).

References

Azetsu-Scott, K., E. P. Jones, I. Yashayaev, and R. M. Gershey, Time series study of CFC concentrations in the Labrador Sea during deep and shallow convection regimes, *J. Geophys. Res., 108*, 3354, doi:10.1029/2002JC001317, 2003.

Azetsu-Scott, K., E. P. Jones, and R. M. Gershey, Distribution and ventilation of water masses in the Labrador Sea inferred from CFCs and Carbon Tetrachloride, *Marinechemistry*, in press.

Barnier, B., L. Siefridt, and P. Marchesiello, Thermal forcing for a global ocean circulation model using a three year climatology of ECMWF analysis, *J.Mar. Sys., 6*, 363-380, 1995.

Beckmann, A., and R. Döscher, A method for improved representation of dense water spreading over topography in geopotential-coordinate models, *J. Phys. Oceanogr., 27*, 581-591, 1997.

Beismann, J.-O., and B. Barnier, Variability of the meridional overturning circulation of the North Atlantic: sensitivity to overflows of dense water masses, *Ocean Dynamics, 54*, 92-106, doi:10.1007/sl0236-003-00788-x, 2004.

Beismann, J.-O., and R. Redler, Model simulations of CFC uptake in North Atlantic Deep Water: Effects of parameterizations and grid resolution, *J. Geophys. Res., 108*, 3159, doi:10.1029/2001JC001253, 2003.

Bell, M. J., M. J. Martin, and N. K. Nichols, Assimilation of data into an ocean model with systematic errors near the equator, *Q. J. R. Meteorol. Soc., 130*, 873-893, doi:10.1256/qj.02.109, 2004.

Böning, C. W., F. O. Bryan, W. R. Holland, and R. Döscher, Deep-water formation and meridional overturning in a high-resolution model of the North Atlantic, *J. Phys. Oceanogr., 26*, 1142-1164, 1996.

Böning, C. W., M. Rhein, J. Dengg, and C. Dorow, Modeling CFC inventories and formation rates of Labrador Sea Water, *Geophys. Res. Lett.*, 30, 1050, doi:10.1029/2002GL014855, 2002.

Bower, A. S., and H. D. Hunt, Lagranging observations of the Deep West Boundary Current in the North Atlantic Ocean. Part I: Large-scale pathways and spreading rates, *J. Phys. Oceanogr., 30*, 764-783, 2000.

Boyer, T. P., and S. Levitus, Objective analyses of temperature and salinity for the world ocean on a 1/4 grid, *NOAA Atlas NESDIS 11*, U.S. Gov. Printing Office, Washington, D.C., 1997.

Bullister, J. L., Chlorofluorocarbons as time-dependent tracers in the ocean, *Oceanography, November*, 12-17, 1989.

Caldeira, K., and P. B. Duffy, Sensitivity of simulated CFC-11 distributions in a global ocean model to the treatment of salt rejected during sea-ice formation, *Geophys. Res. Lett., 25*, 1003-1006, 1998.

Dengg, J., C. Böning, U. Ernst, R. Redler, and A. Beckmann, Effects of an improved model representation of overflow water on the subpolar North Atlantic, *International WOCE Newsletter, 37*, 10-15, 1999.

Dixon, K. W., J. L. Bullister, R. H. Gammon and R. J. Stouffer, Examining a coupled climate model using CFC-11 as an ocean tracer, *Geophys. Res. Lett., 23*, 1957-1960, 1996.

Doney, S. C., and W. J. Jenkins, Ventilation of the Deep Western Boundary Current and abyssal western North Atlantic: Estimates from tritium and ^3H_e distributions, *J. Phys. Oceanogr., 24*, 638-659, 1994.

Döscher, R., and R. Redler, The relative importance of northern overflow and subpolar deep convection for the North Atlantic thermohaline circulation, *J. Phys. Oceanogr., 27*, 1894-1902, 1997.

Döscher, R., C. Böning, and P. Herrmann, Response of circulation and heat transport in the North Atlantic to changes in thermohaline forcing in northern latitudes: A model study, *J. Phys. Oceanogr., 24*, 2306-2320, 1994.

Dutay, J. -C., and Coauthors, Evaluation of ocean model ventilation with CFC-11: comparison of 13 global ocean models, *Ocean Modelling, 4*, 89-120, 2002.

The DYNAMO-group, Dynamics of the North Atlantic Circulation: Simulation and assimilation with high-resolution models, *Technical Report*, Ber. Institut für Meereskunde, Universität Kiel, 1997.

Eden, C., and R. J. Greatbatch, A damped, decadal oscillation in the North Atlantic climate system, *J. Climate, 16*, 4043-4060, 2003.

Eden, C., and T. Jung, North Atlantic interdecadal variability: oceanic response to the North Atlantic Oscillation (1865-1997), *J. Climate, 14*, 676-691, 2001.

Eden, C., and J. Willebrand, Mechanism of interannual to decadal variability of the North Atlantic circulation, *J. Climate, 14*, 2266-2280, 2001.

Eden, C., R. J. Greatbatch, and C. Böning, Adiabatically correcting an eddy-permitting model using large-scale hydrographic data: Application to the Gulf Stream and the North Atlantic Current, *J. Phys. Oceanogr., 34*, 701-719, 2004.

England, M. H., Using chlorofluorocarbon to assess ocean climate models, *Geophys. Res. Lett., 22*, 3051-3054, 1995.

England, M. H., and A. C. Hirst, Chlorofluorocarbon uptake in a world ocean model. 2. Sensitivity to surface thermohaline forcing and subsurface mixing parameterizations, *J. Geophys. Res., 102*, 15709-15731, 1997.

England, M. H., and G. Holloway, Simulations of CFC content and water mass age in the deep North Atlantic, *J. Geophys. Res., 103*, 15885-15901, 1998.

England, M. H., V.Garcon, and J.-F. Minster, Chlorofluorocarbon uptake in a world ocean model. 1. Sensitivity to the surface gas forcing, *J. Geophys. Res., 99*, 25215-25233, 1994.

Fine, R. A., and R. L. Molinari, A continuous deep western boundary current between Abaco (26.5°N) and Barbados (13°N), *Deep-Sea Res., 35*, 1441-1450, 1988.

Fine, R. A., M. Rhein and C.Andrié, Using a CFC effective age to estimate propagation and storage of climate anomalies in the deep western North Atlantic Ocean, *Geophys. Res. Lett., 29*, 2227, doi:10.1029/2002GL015618, 2002.

Gaspar, P., Y. Gregoris, and J.-M. Lefevre, A simple eddy kinetic energy model for simulation of the oceanic vertical mixing: tests at station PAPA and Long-Term Upper Ocean Study site, *J. Geophys. Res., 95*, 16179-16193, 1990.

Gent, P. R., and J. C. McWilliams, Isopycnal mixing in ocean circulation models, *J. Phys. Oceanogr., 20*, 150-155, 1990.

Greatbatch, R. J., The North Atlantic Oscillation, *Stochastic Environmental Research and Risk Assessment*, 14 (4+5), 213-242, 2000.

Greatbatch, R. J., J. Sheng, C. Eden, L. Tang, X. Zhai and J. Zhao, The semi-prognostic method. *Continental Shelf Research*, 24/18, 2149-2165, 2004.

Haine, T. W. N., and K. J. Richards, The influence of the seasonal mixed layer on oceanic uptake of CFCs, *J. Geophys. Res., 100*, 10727-10744, 1995.

Haine, T. W. N., K. J. Richards, and Y. Jia, Chlorofluorocarbon constraints on North Atlantic Ventilation, *J. Phys. Oceanogr., 33*, 1798-1814, 2003.

Hurrell, J.W., Y. Kushnir, G. Ottersen, and M. Visbeck, An Overview of the North Atlantic Oscillation, *The North Atlantic Oscillation, Geophysical Monograph Series*, 1-35, 2003.

Johns, W. E., D. M. Fratantoni, and R. J. Zantopp, Deep Western Boundary Current variability off northeastern Brazil, *Deep Sea Res., 40*, 293-310, 1993.

Kalnay, E., and Coauthors, The NCEP/NCAR 40-year reanalysis project, *Bull. Amer. Meteor. Soc., 77*, 437-472, 1996.

Kieke, D., M. Rhein, L. Stramma, W. M. Smethie, D. A. LeBel, and W. Zenk, Changes in the CFC inventories and formation rates of Upper Labrador Sea Water, 1997-2001, *J. Phys. Oceanogr.*, submitted, 2004.

Lazier, J.R.N., Observations in the northwest corner of the North Atlantic current, *J. Phys. Oceanogr., 24*, 1449-1463, 1994.

Leetmaa, A., P. Niiler, and H. Stommel, Does the Sverdrup relation account for the mid-Atlantic circulation?, *J. Mar. Res., 35*, 1-10, 1977.

Levitus, S., and T. P. Boyer, World Ocean Atlas 1994, *Tec. Rep.*, NOAA, 1994.

Oschlies, A., and V. Garcon, An eddy-permitting coupled physical-biological model of the North Atlantic. 1. Sensitivity to advection numerics and mixed layer physics, *Glob. Biochem. Cycles, 13*, 135-160, 1999.

Redi, M. H., Oceanic isopycnal mixing by coordinate rotation, *J. Phys. Oceanogr., 12*, 1154-1158, 1982.

Rhein, M., The Deep Western Boundary Current: Tracers and velocities, *Deep Sea Res., 41*, 263-281, 1994.

Robitaille, D. Y. and A. J. Weaver, Validation of sub-grid-scale mixing schemes using CFCs in a global ocean model, *Geophys. Res. Lett., 35*, 2917-2920, 1995.

Rogers, J. C., The association between the North Atlantic Oscillation and the Southern Oscillation in the Northern Hemisphere, *Mon. Wea. Rev., 112*, 1999-2015, 1984 .

Schott, F., J. Fisher, J. Reppin, and U. Send, On mean and seasonal currents and transports at the western boundary of the equatorial Atlantic, *J. Geophys. Res., 98*, 14353-14368, 1993.

Sheng, J., R. J. Greatbatch, and D. G. Wright, Improving the utility of ocean circulation models through adjustment of the momentum balance, *J. Geophys. Res., 106*, 16,711-16,728, 2001.

Smethie Jr., W. M., Tracing the thermohaline circulation in the western North Atlantic using chlorofluorocarbons, *Prog. Oceanogr., 31*, 51-99, 1993.

Smethie Jr., W. M., Meridional distribution of CFCs in the western subtropical Atlantic Ocean, *International WOCE newsletter, 37*, 15-17, 1999.

Smethie Jr., W. M., and R. Fine, Rates of North Atlantic Deep water formation calculated from chlorofluorocarbon inventories, *Deep-Sea Res., 48*, 189-215, 2001.

Smethie Jr., W. M., R. A. Fine, A. Putzka, and E. P. Jones, Tracing the flow North Atlantic Deep Water using chlorofluorocarbons, *J. Geophys. Res., 105*, 14297-14323, 2000.

Tait, V. K., R. M. Gershey, and E. P. Jones, Inorganic carbon in the Labrador Sea: Estimation of the anthropogenic component, *Deep-Sea Res. I, 47*, 295-308, 2000.

Visbeck, M., E. P. Chassignet, R. G. Curry, T. L. Delworth, R. R. Dickson, and G. Krahmann, The ocean's response to North Atlantic Oscillation variability, *AGU Geophysical monograph 134: The North Atlantic Oscillation*, 10.1029/134GM06, 113-145, 2003.

Walker, S. J., R. F. Weiss, and P. K. Salameh, Reconstructed histories of the annual mean atmospheric mole fractions for the halocarbons CFC-11, CFC-12, CFC-113, and carbon tetrachloride, *J. Geophys. Res., 105*, 14285-14296, 2000.

Wanninkhof, R., Relationship between wind speed and gas exchange over the ocean, *J. Geophys. Res., 97*, 7373-7382, 1992.

Warner, M. J. and R. F. Weiss, Solubilities of chlorofluorocarbons 11 and 12 in water and seawater, *Deep sea Res., Part A, 32*, 1485-1497, 1985.

Weiss, R. F., J. L. Bullister, R. H. Gammon, and M. J. Warner: Atmospheric chlorofluoromethanes in the deep equatorial Atlantic, *Nature, 314*, 608-610, 1985.

Williams, R. T., Transient tracers in the ocean, tropical Atlantic study data report, *Tech. Rep. Ref., 86-16*, Scripps Inst. of Oceanogr, 300 pp., 1986.

Zhai, X., R. J. Greatbatch, and J. Sheng, Diagnosing the role of eddies in driving the circulation of the Northwest Atlantic Ocean, *Geophys. Res. Lett.*, in press, 2004.

Zhao, J., R. J. Greatbatch, J. Sheng, C. Eden, and K. Azetsu-Scott, Impact of an adiabatic correction technique on the simulation of CFC-12 in a model of the North Atlantic Ocean, *Geophys. Res. Lett., 31*, L12309, doi:10.1029/2004GL020206, 2004.

Received _____; accepted .

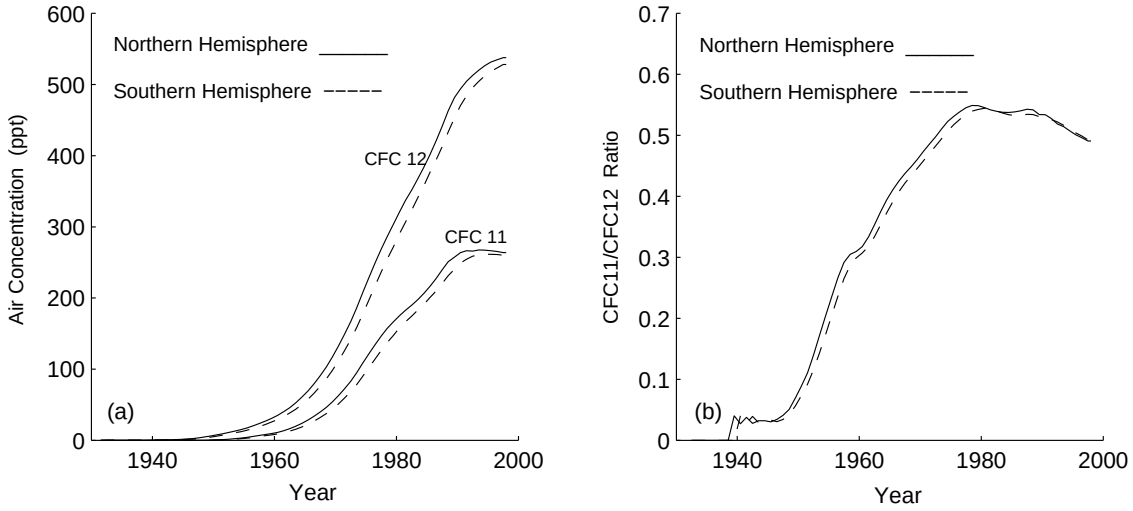

Figure 1: Time-series of (a) CFC-11 and CFC-12 atmospheric concentrations in units of ppt (parts per trillion), and (b) the ratio of CFC-11 to CFC-12 in the Northern and Southern Hemispheric tropospheres (adopted from Walker et al. [2000]).

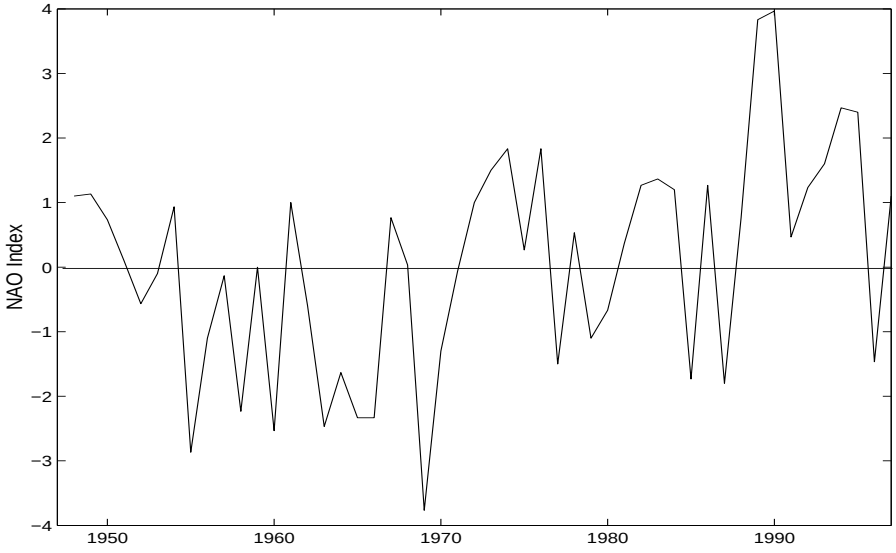

Figure 2: Time-series of the observed winter (January-February-March) NAO index from 1948 to 1997 [Eden and Jung, 2001].

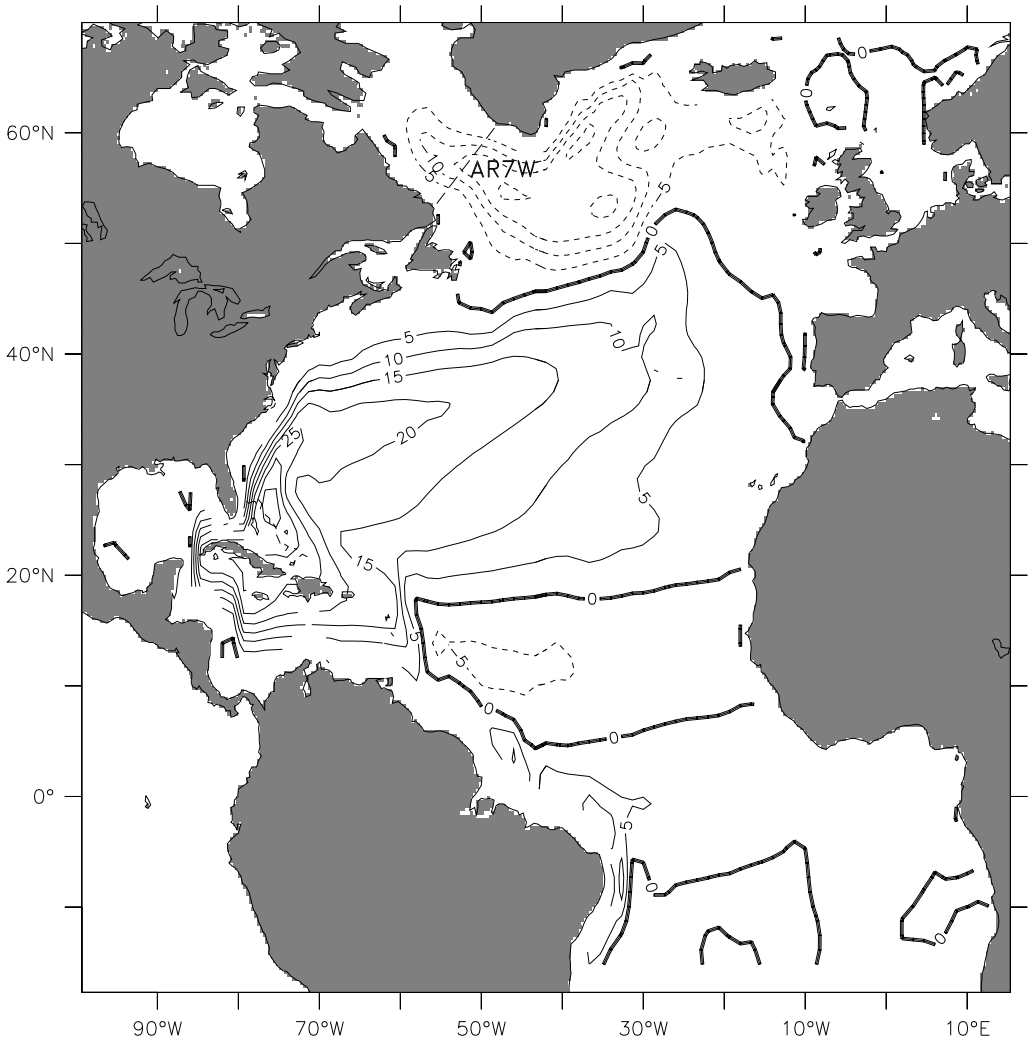

Figure 3: Time-mean volume transport streamfunction calculated from the 50-year (1948-1997) model run in experiment NAO-sp. The contour intervals is 5 Sv (1 Sv=10^6 m^3 s^{-1}). Solid (dashed) lines denote positive (negative) values of the transport streamfunction. The zero contour is highlighted. Also shown is the WOCE AR7W line (see text).

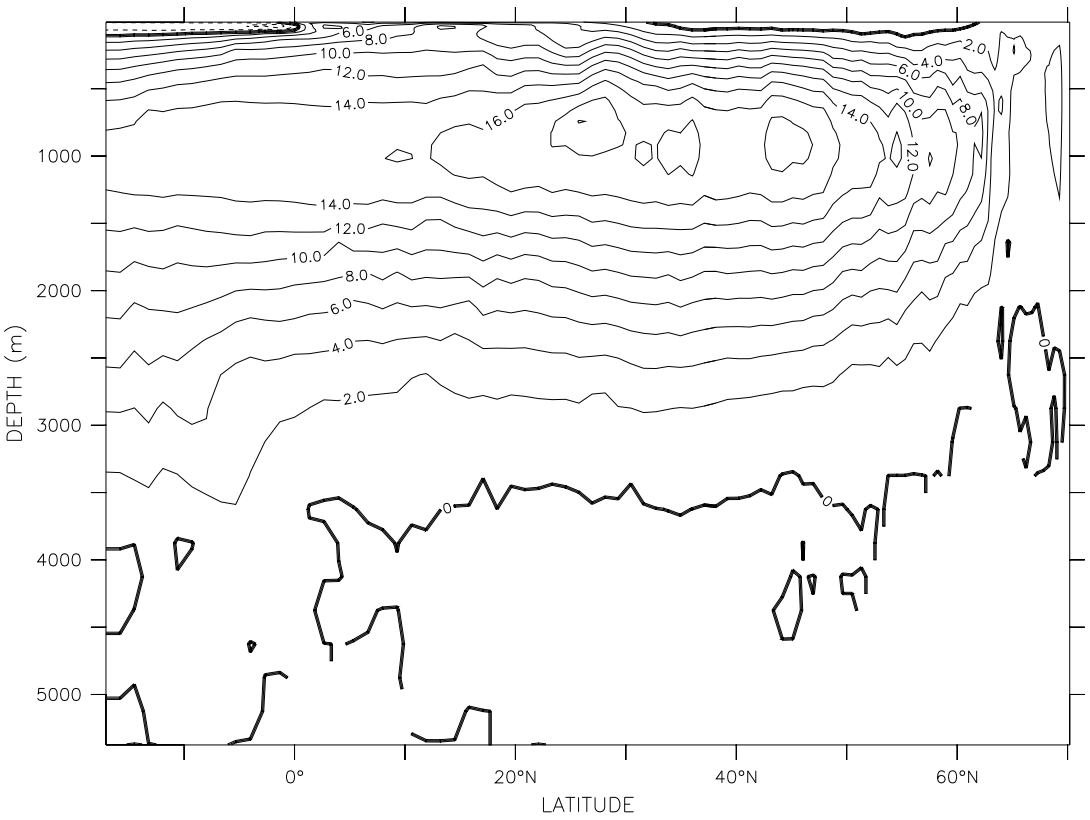

Figure 4: Time-mean meridional overturning streamfunction calculated from the 50-year (1948-1997) model run in experiment NAO-sp. The contour interval is 1 Sv.

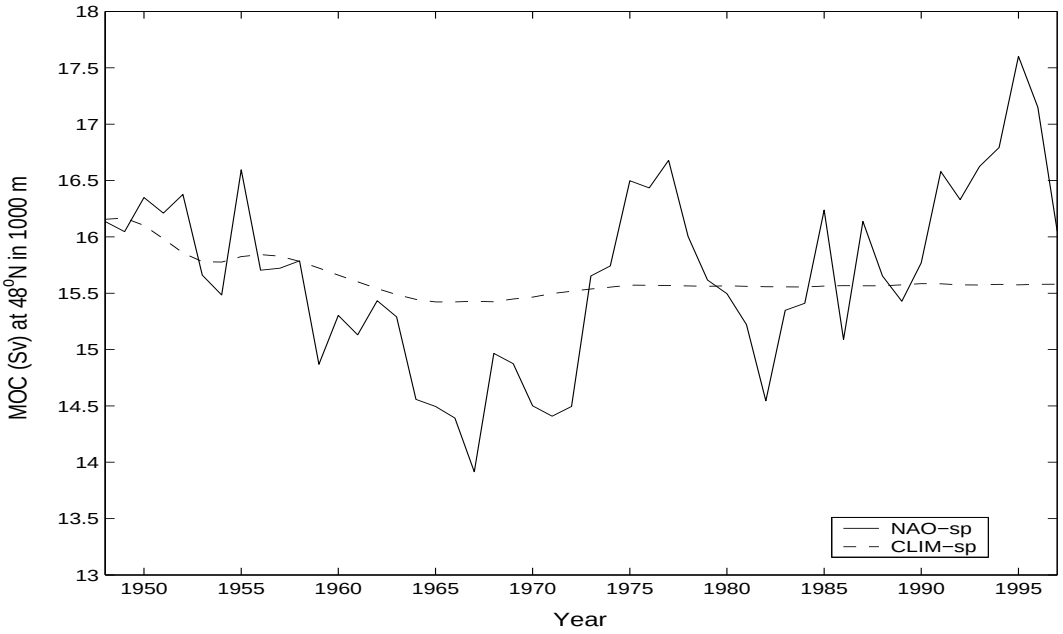

Figure 5: Comparison of the annual mean overturning streamfunctions at 48° N and 1000 m depth in each of experiments NAO-sp (solid) and CLIM-sp (dashed).

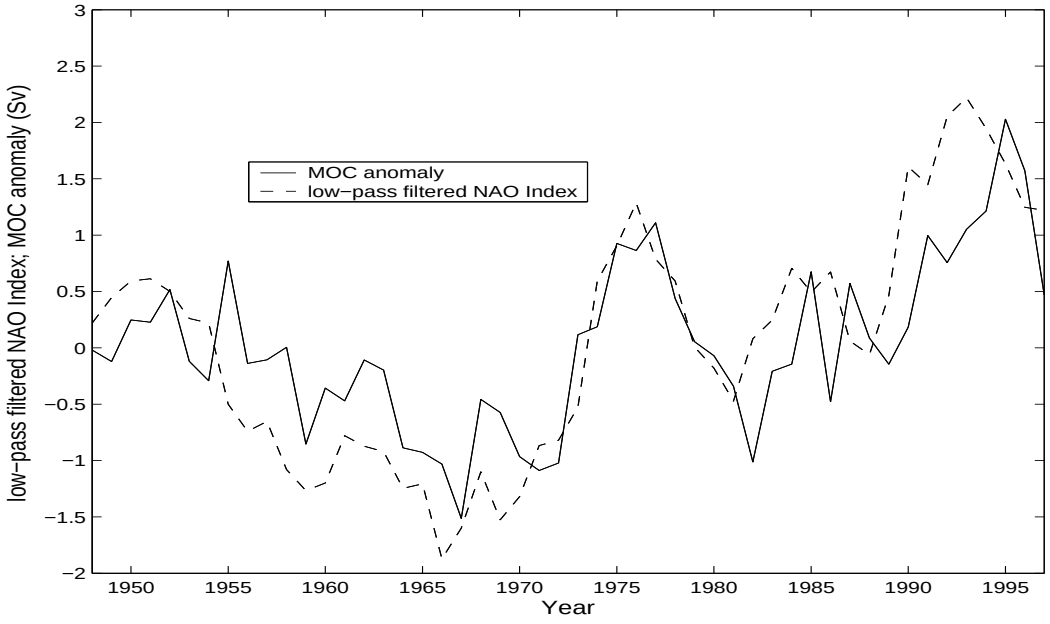

Figure 6: Time series of the low-pass filtered winter-mean (JFM) NAO index (dashed) and the unfiltered anomaly of the annual mean overturning streamfunction at 48° N at 1000 m (solid) produced by the model in experiment NAO-sp.

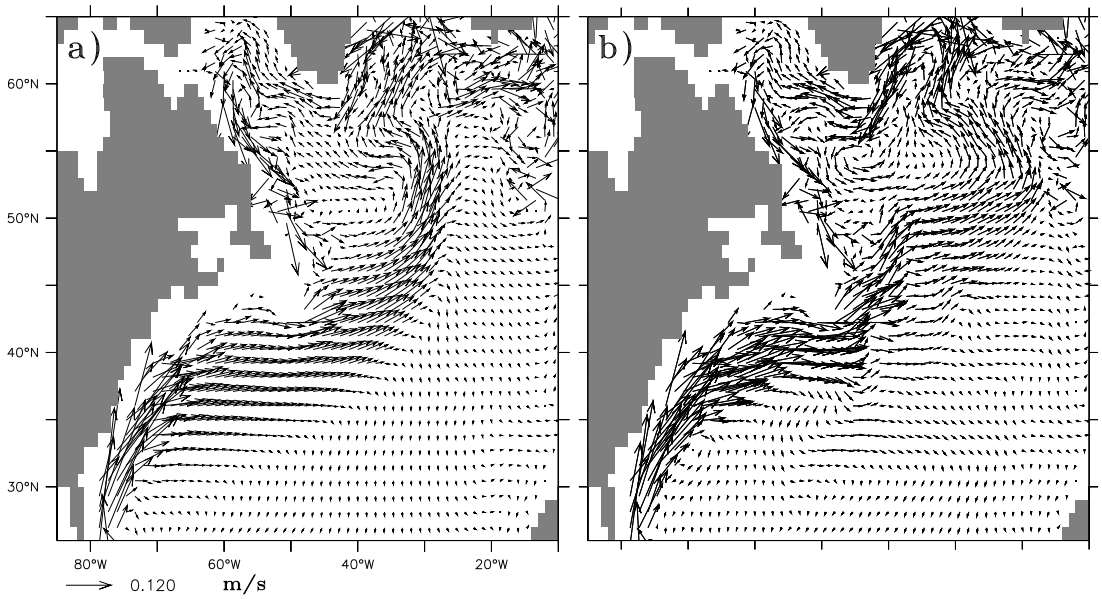

Figure 7: Time-mean circulation at 200 m calculated from the 50-year (1948-1997) model run in each of experiments (a) CLIM-pp, and (b) CLIM-sp.

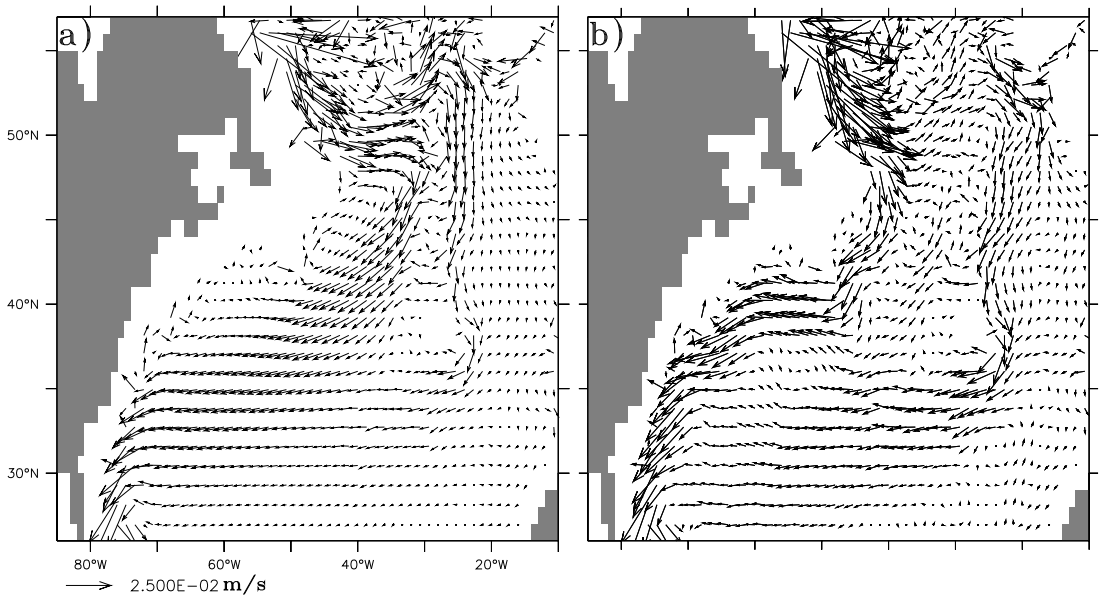

Figure 8: Time-mean circulation at 1500 m calculated from the 50-year (1948-1997) model run in each of experiments (a) CLIM-pp, and (b) CLIM-sp.

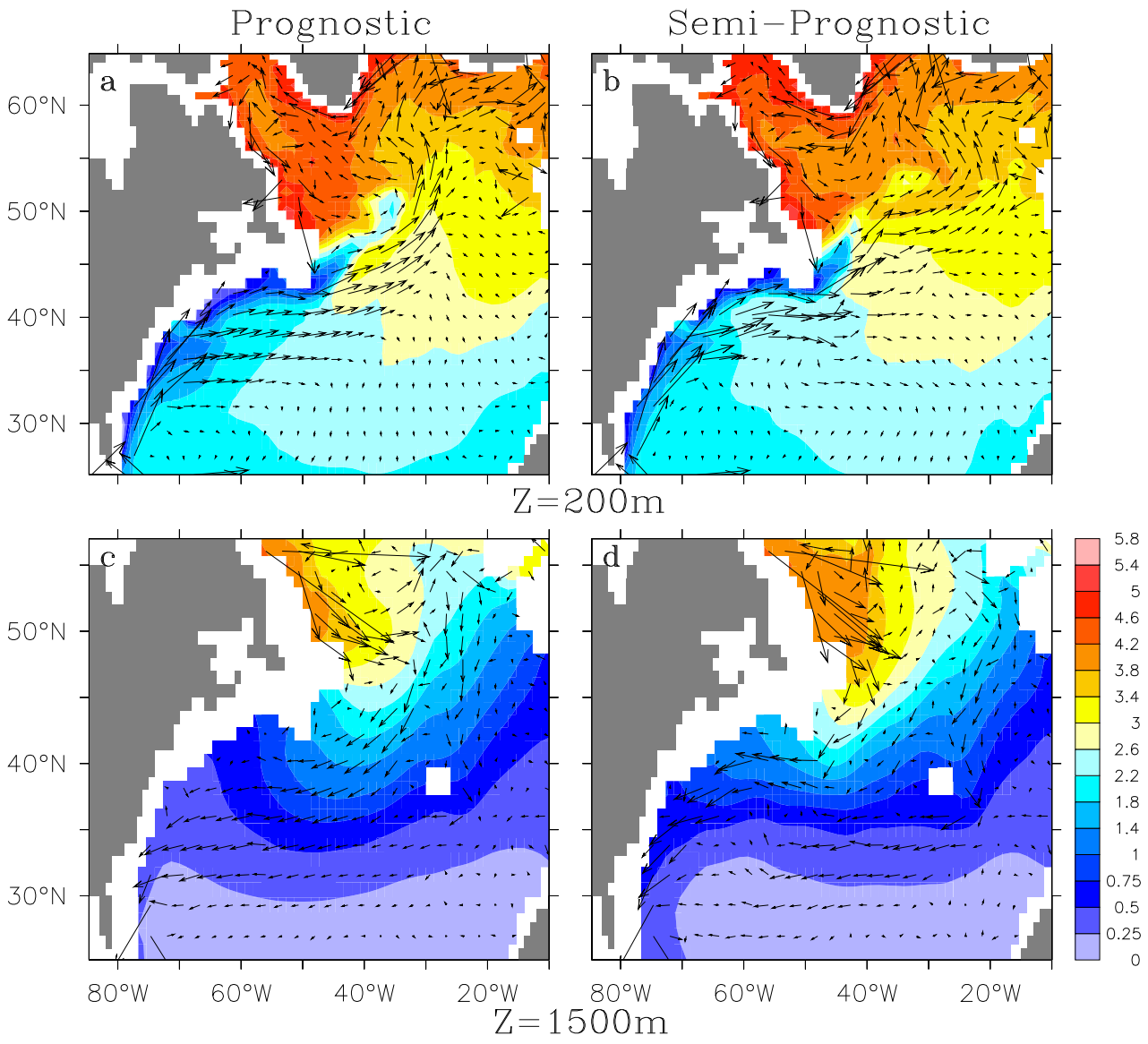

Figure 9: Monthly mean CFC-11 concentration in pmol kg^{-1} (color image) and horizontal velocity (arrows) over the western subtropical Atlantic in February 1990 at 200 m in experiments (a) CLIM-pp and (b) CLIM-sp. (c) and (d) are as for (a) and (b) but at 1500 m.

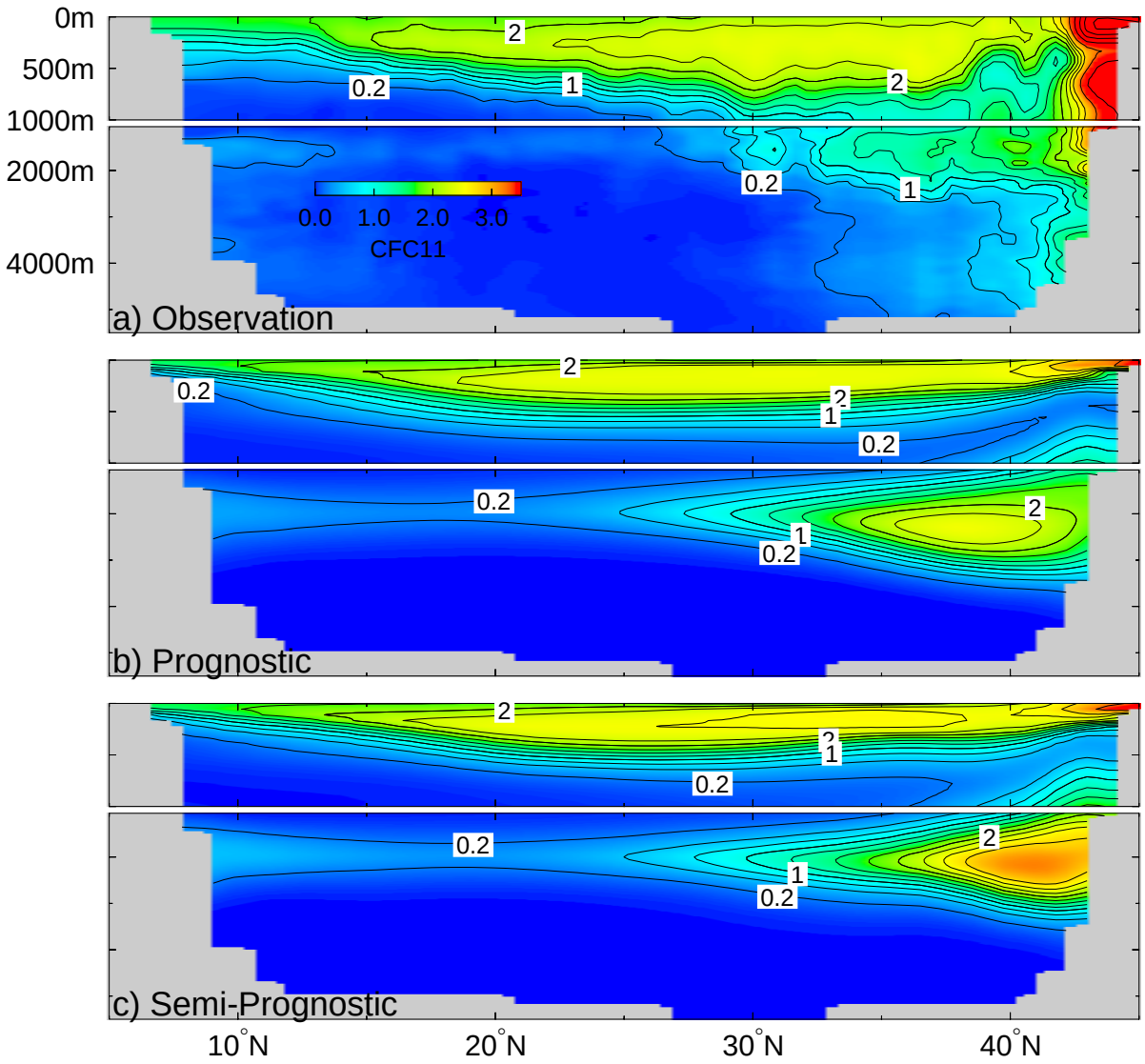

Figure 10: (a) The observed CFC-11 concentration in pmol kg^{-1} along a meridional transect A20 at 52° W in the North Atlantic in July/August of 1997 interpolated from the data set described by Smethie et al. [2000]. The 2-month mean CFC-11 concentrations in pmol kg^{-1} averaged from the model results over July and August of 1997 along the same transect using (b) the prognostic (uncorrected) model and (c) the modified semi-prognostic model.

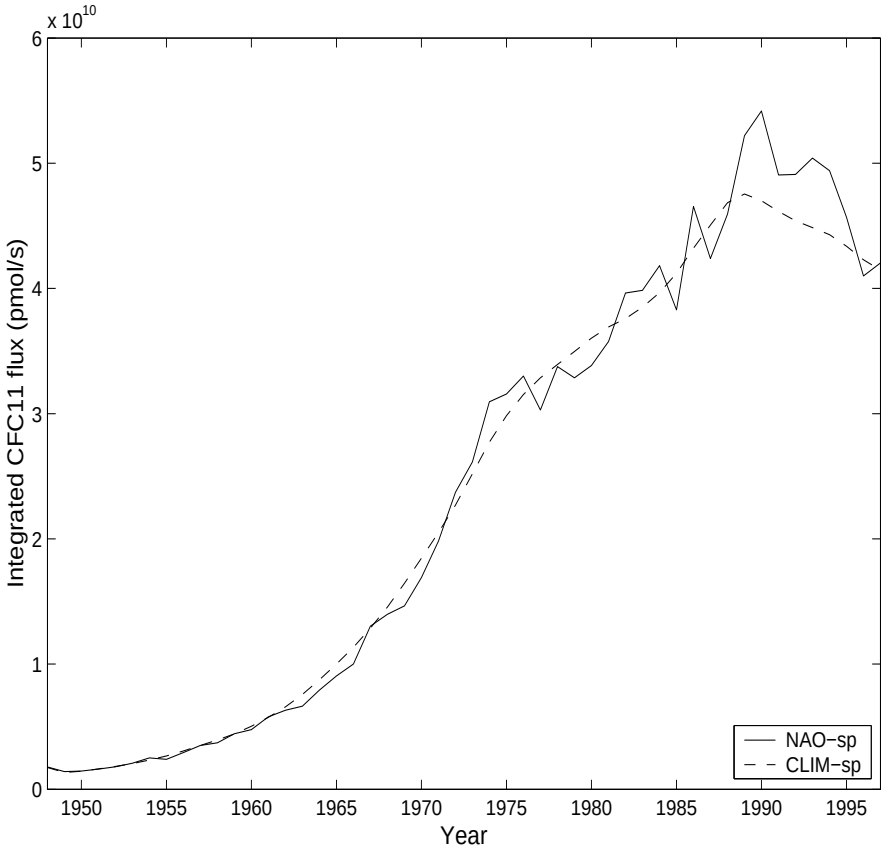

Figure 11: Time series of the annual mean surface flux of CFC-11 (pmol s^{-1}) over the Labrador Sea region (43° W-60° W, 49° N-64° N) in experiments NAO-sp (solid) and CLIM-sp (dashed).

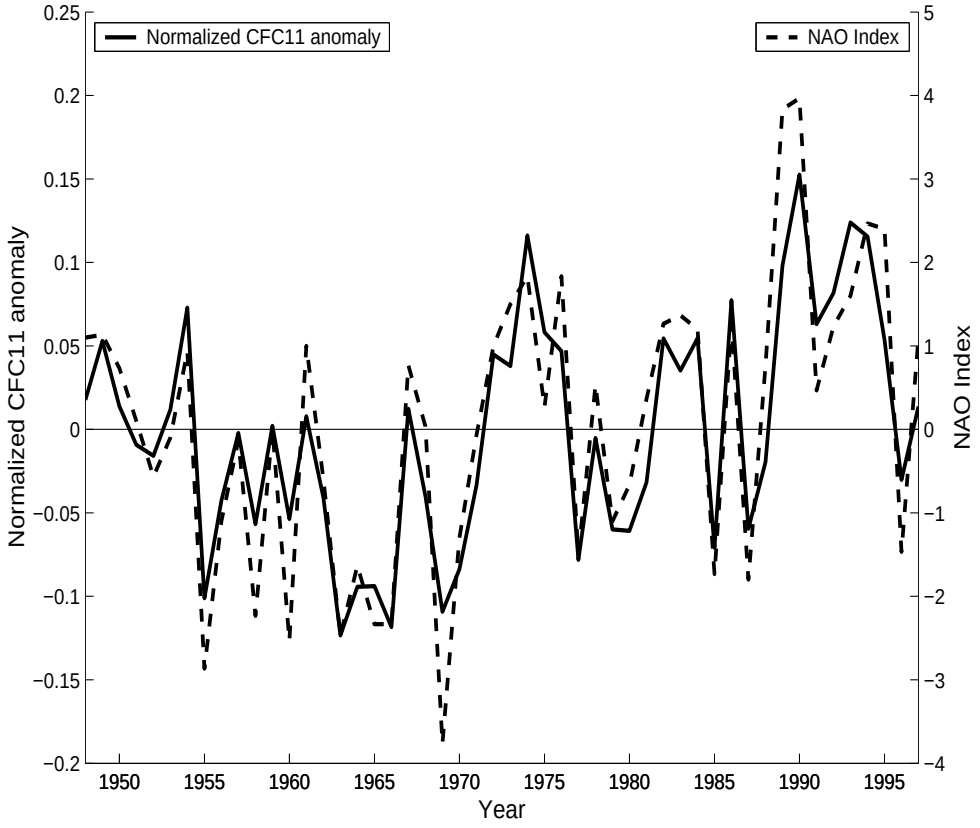

Figure 12: (a) Time-series of the normalized anomaly (solid) in the annual mean surface flux of CFC-11 over the Labrador Sea region, and the winter-mean NAO index (dashed).

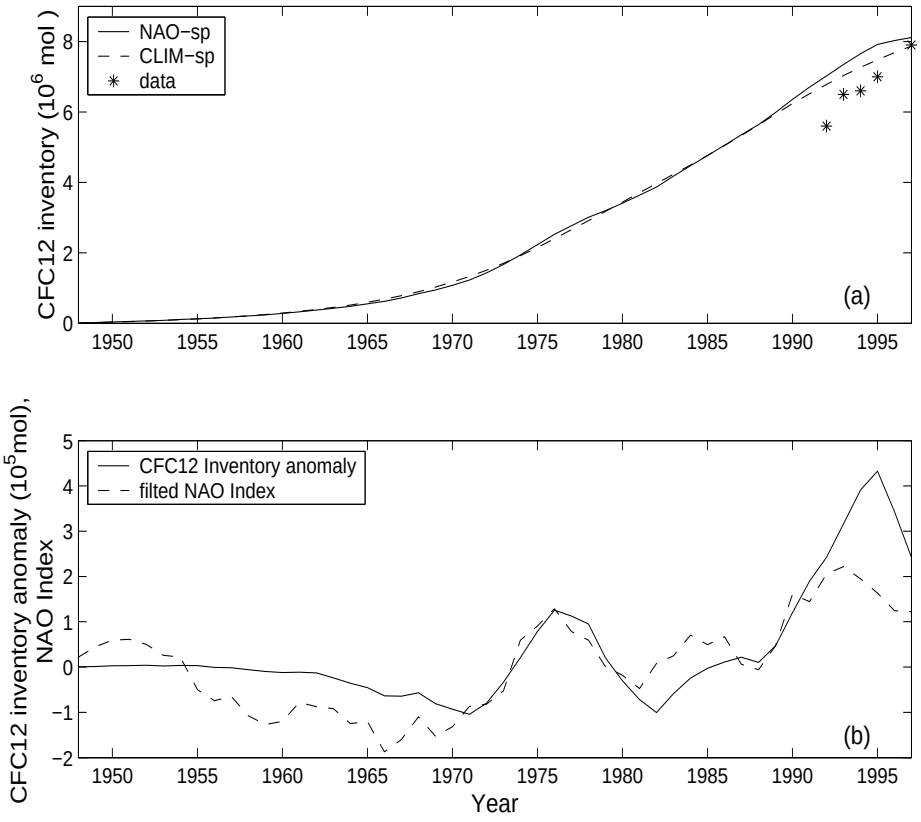

Figure 13: (a) The inventory of CFC-12 in the Labrador Sea region (43° W-60° W, 49° N-64° N) calculated from experiments NAO-sp (solid line) and CLIM-sp (dashed line), and estimated from observations (stars) by Azetsu-Scott et al. [2003]; (b) The model-calculated anomaly of CFC-12 inventory (solid line) and the low-pass filtered winter-mean NAO index (dashed line).

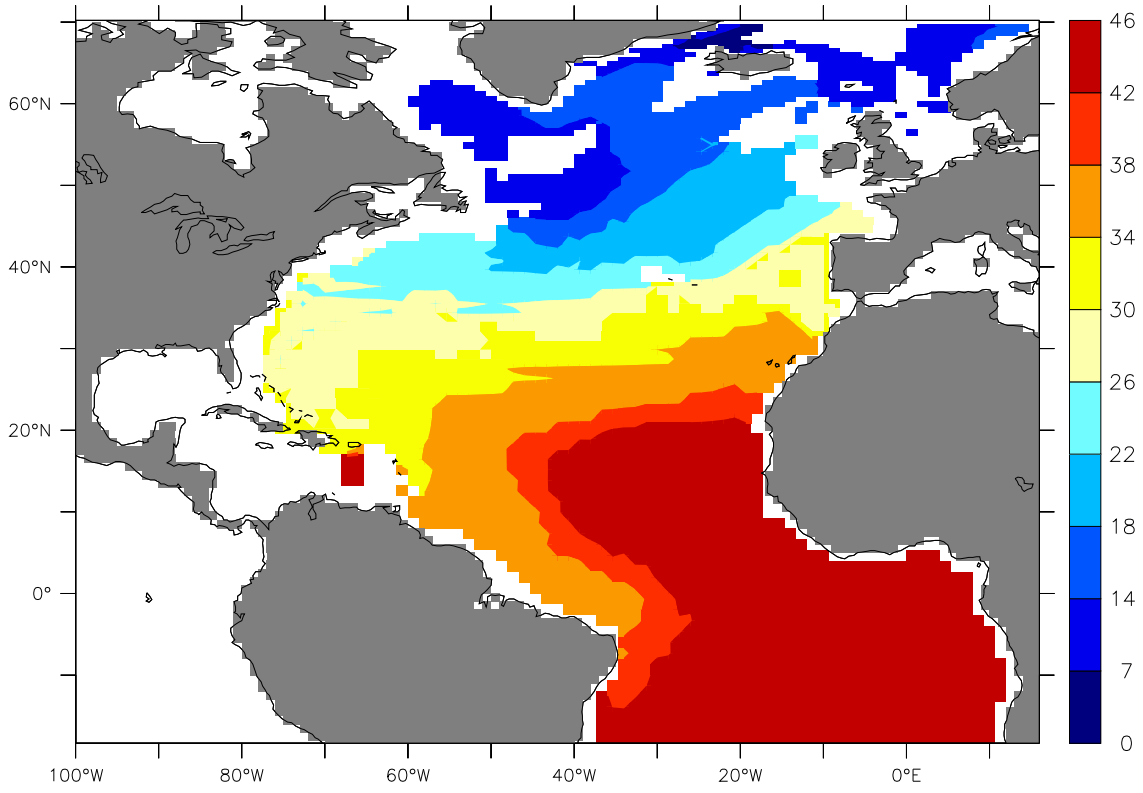

Figure 14: Annual mean pCFC-11 age (in years) in 1997 along the isopycnal surface $\sigma_0 = 27.8$ *kg/m*^{3} *for Labrador Sea Water calculated from experiment CLIM-sp.*

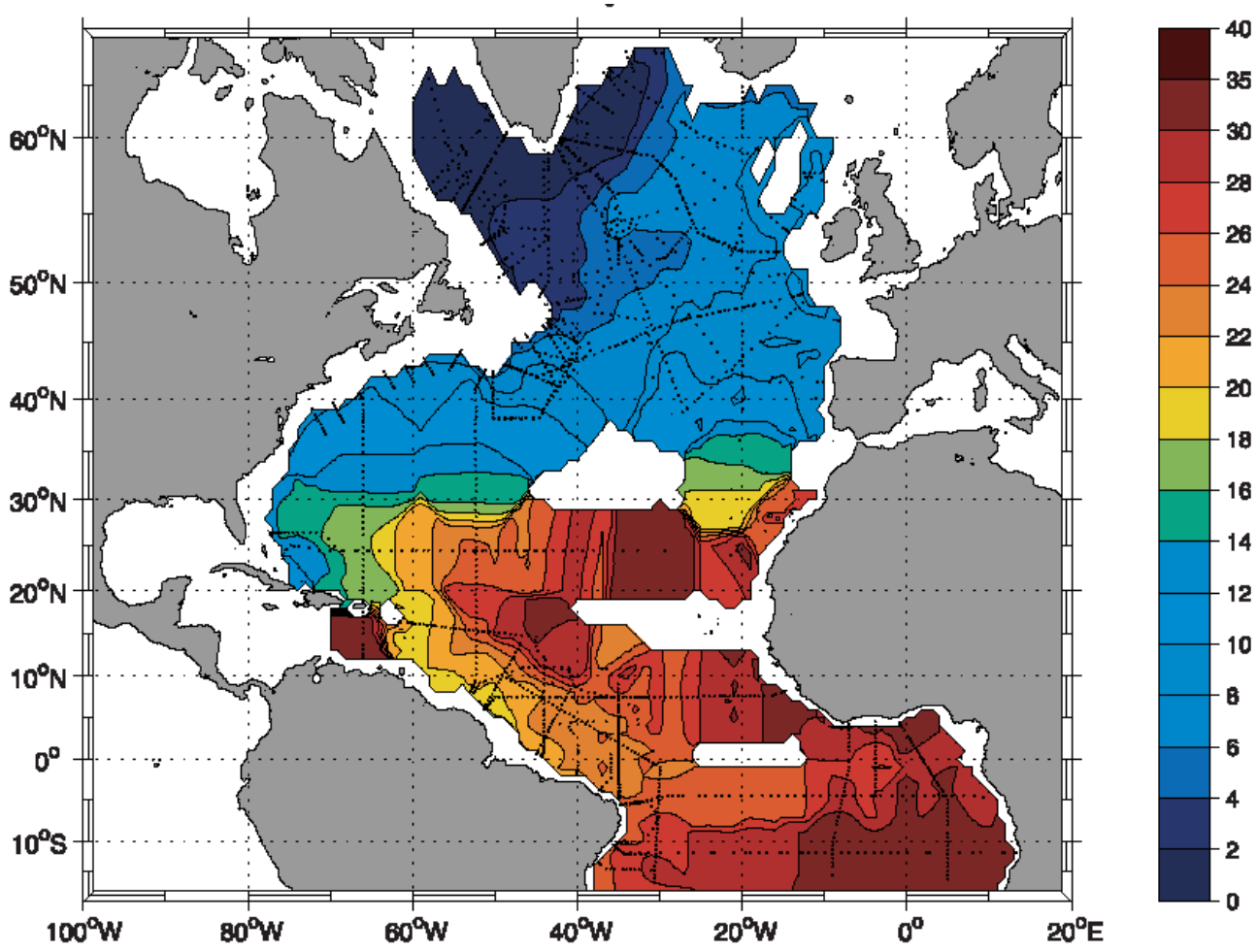

Figure 15: Distribution of CFC-11 effective age (year) on σ_0=27.78 kg/m^3 in 1997, with the "relic" age of 15 years subtracted from the pCFC-11 age, and estimated from observed CFC-11 concentrations collected during the 1990s. Station locations are shown by black dots. The contour interval is 2 years. (Adopted from Fine et al. [2002]).

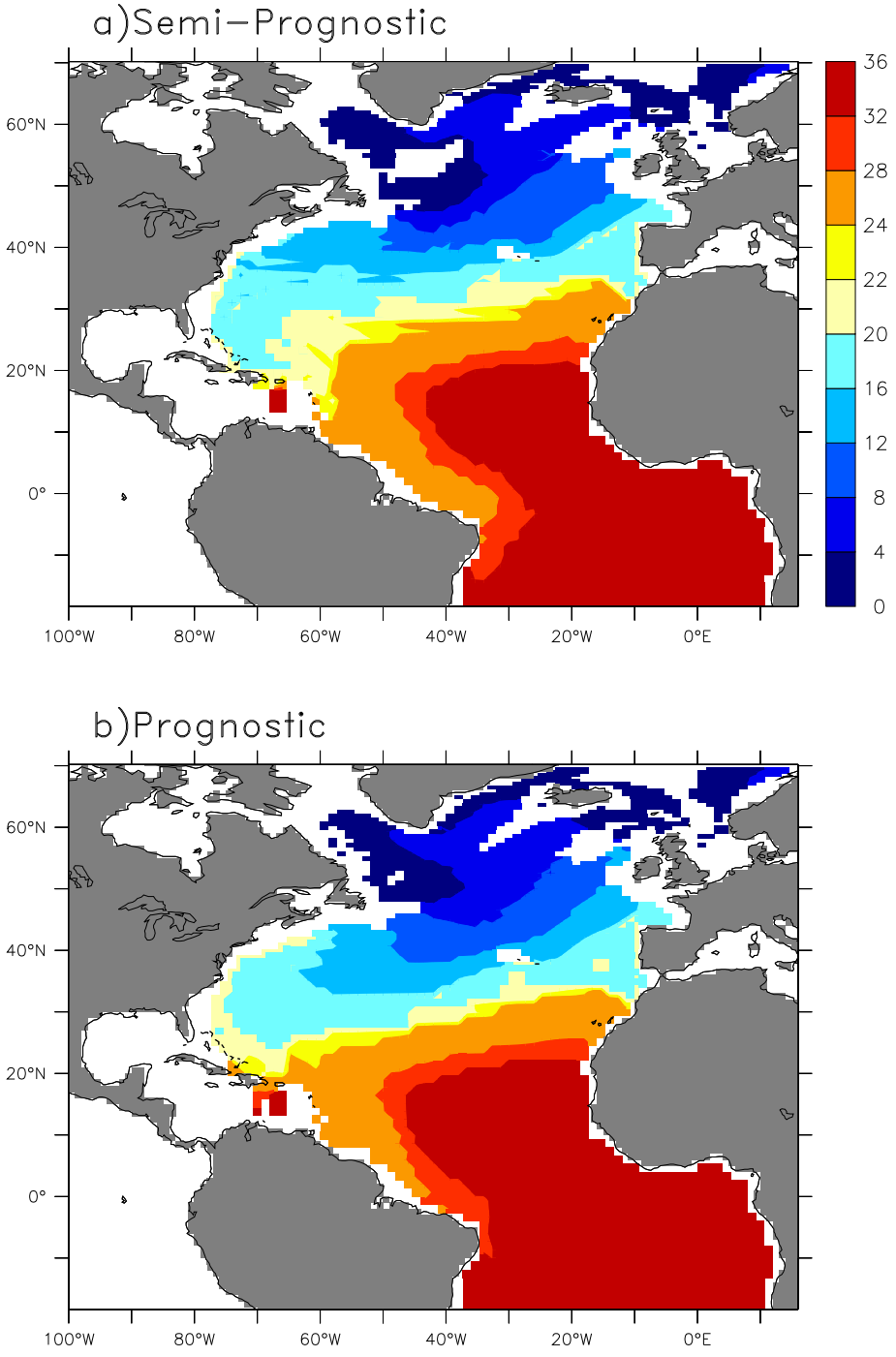

Figure 16: CFC-11 effective age (in years) on the isopycnal surface σ_0=27.8 kg/m^3 in 1997, with the "relic" age of 14 years subtracted, calculated from experiments (a) CLIM-sp and (b) CLIM-pp.